

Aberystwyth University

Meltwater export of prokaryotic cells from the Greenland ice sheet

Cameron, Karen; Stibal, Marek; Hawkings, Jon; Mikkelsen, Andreas; Telling, Jon; Kohler, Tyler J.; Gözdereliler, Erkin; Zarsky, Jakub D.; Wadham, Jemma L.; Jacobsen, Carsten

Published in:
Environmental Microbiology

DOI:
[10.1111/1462-2920.13483](https://doi.org/10.1111/1462-2920.13483)

Publication date:
2017

Citation for published version (APA):
Cameron, K., Stibal, M., Hawkings, J., Mikkelsen, A., Telling, J., Kohler, T. J., ... Jacobsen, C. (2017). Meltwater export of prokaryotic cells from the Greenland ice sheet. *Environmental Microbiology*, 19(2), 524-534.
<https://doi.org/10.1111/1462-2920.13483>

General rights

Copyright and moral rights for the publications made accessible in the Aberystwyth Research Portal (the Institutional Repository) are retained by the authors and/or other copyright owners and it is a condition of accessing publications that users recognise and abide by the legal requirements associated with these rights.

- Users may download and print one copy of any publication from the Aberystwyth Research Portal for the purpose of private study or research.
- You may not further distribute the material or use it for any profit-making activity or commercial gain
- You may freely distribute the URL identifying the publication in the Aberystwyth Research Portal

Take down policy

If you believe that this document breaches copyright please contact us providing details, and we will remove access to the work immediately and investigate your claim.

tel: +44 1970 62 2400
email: is@aber.ac.uk

1 **Title: Meltwater export of prokaryotic cells from the Greenland Ice Sheet**

2

3 Karen A Cameron^{1,2}, Marek Stibal^{1,2,3}, Jon R Hawkings⁴, Andreas B Mikkelsen², Jon Telling⁴,

4 Tyler J Kohler³, Erkin Gözdereliler^{1,2}, Jakub D Zarsky³, Jemma L Wadham⁴, Carsten S

5 Jacobsen^{2,5}

6

7 ¹Department of Geochemistry, Geological Survey of Denmark and Greenland (GEUS),

8 Copenhagen, Denmark

9 ²Center for Permafrost (CENPERM), University of Copenhagen, Copenhagen, Denmark

10 ³Department of Ecology, Charles University in Prague, Prague, Czech Republic

11 ⁴Bristol Glaciology Centre, School of Geographical Sciences, University of Bristol, UK

12 ⁵Department of Environmental Science, Aarhus University, Roskilde, Denmark

13

14

15 Corresponding author: Dr. Karen A. Cameron, Department of Geochemistry, Geological

16 Survey of Denmark and Greenland (GEUS), Øster Voldgade 10, 1350 Copenhagen K,

17 Denmark. Telephone: +44 7764 968 773, fax: na, email: kac.geus@gmail.com,

18

19

20 Running head: Microbial export from the Greenland Ice Sheet

21 Type of paper: Research Article

22 Originality-Significance Statement:

23 This study is the first to consider the flux of microbial assemblages from the Greenland Ice
24 Sheet (GrIS) to downstream ecosystems. We estimate that 10^{21} prokaryotic cells, equivalent to
25 ~ 31 Mg of carbon, were transported from the studied catchment area in 2012. When upscaled
26 to estimated cell flux associated with freshwater runoff from the entire GrIS, we estimate that
27 $\sim 6.3 \times 10^{22}$ cells yr^{-1} , or ~ 1900 Mg yr^{-1} of carbon is released, which is at least seventeen times
28 lower than the yearly contribution of prokaryotic cells from the four largest rivers that feed
29 the Arctic Ocean. Biomass release scaled with discharge, and community compositions were
30 temporally and spatially stable, indicating that the sampled river microbiota were
31 predominantly of glacial origin. GrIS annual freshwater flux, and the areas affected by
32 hydrological activity are predicted to increase as a result of climate warming. These results
33 therefore indicate that elevated biomass release should similarly be anticipated in the future.
34 The ecological implications of this are now timely to consider.

35

36 Summary:

37 Microorganisms are flushed from the Greenland Ice Sheet (GrIS) where they may contribute
38 towards the nutrient cycling and community compositions of downstream ecosystems. We
39 investigate meltwater microbial assemblages as they exit the GrIS from a large outlet glacier,
40 and as they enter a downstream river delta during the record melt year of 2012. Prokaryotic
41 abundance, flux and community composition was studied, and factors affecting community
42 structures were statistically considered. The mean concentration of cells exiting the ice sheet
43 was 8.30×10^4 cells ml^{-1} and we estimate that $\sim 1.02 \times 10^{21}$ cells were transported to the
44 downstream fjord in 2012, equivalent to 30.95 Mg of carbon. Prokaryotic microbial
45 assemblages were dominated by Proteobacteria, Bacteroidetes and Actinobacteria. Cell
46 concentrations and community compositions were stable throughout the sample period, and

47 were statistically similar at both sample sites. Based on our observations, we argue that the
48 subglacial environment is the primary source of the river-transported microbiota, and that cell
49 export from the GrIS is dependent on discharge. We hypothesise that the release of subglacial
50 microbiota to downstream ecosystems will increase as freshwater flux from the GrIS rises in a
51 warming world.

52

53 **Introduction:**

54 The Greenland Ice Sheet (GrIS) has experienced a significant increase in annual surface melt
55 over the past three decades (Fettweis *et al.*, 2011), with a net ice mass loss over the last two
56 decades (Rignot *et al.*, 2011; Shepherd *et al.*, 2012), largely as the result of rising Arctic air
57 temperatures (Hanna *et al.*, 2008). Meltwater accounts for approximately a third of this mass
58 loss (Bamber *et al.*, 2012), the majority of which gets routed through englacial and subglacial
59 environments by moulins and crevasses (Clason *et al.*, 2015) before emerging from the glacial
60 system (Bartholomew *et al.*, 2011; Chandler *et al.*, 2013). By 2100, the annual freshwater flux
61 from the GrIS is estimated to increase by 200 - 1600 GT yr⁻¹ in comparison to the 1980-1999
62 mean (equivalent to ~2 - 13 cm sea level rise; Fettweis *et al.*, 2012), highlighting the
63 sensitivity of the world's second largest source of frozen freshwater to a changing climate.

64 Recent work has demonstrated the importance of glacial meltwaters in delivering
65 nutrients to the polar oceans (Bhatia *et al.*, 2013; Wadham *et al.*, 2013; Hawkings *et al.*, 2014,
66 2015; Lawson *et al.*, 2014a, b). Projected future increases in meltwater runoff (Fettweis *et al.*,
67 2012) and hydrologically active drainage areas (Leeson *et al.*, 2014) in a warming climate are
68 anticipated to elevate dissolved and particulate material released from subglacial
69 environments (Hudson *et al.*, 2014; Hawkings *et al.*, 2015). Furthermore, anomalous events,
70 such as atypical increases in supraglacial melt and supraglacial lake drainage (Hasholt *et al.*,
71 2006; Bartholomew *et al.*, 2011) may increase in frequency, and influence glacial motion and

72 augment subglacial sediment release (Bartholomew *et al.*, 2011; Hudson *et al.*, 2014). The
73 GrIS has recently experienced several extreme melt events (Comiso, 2006; Tedesco, 2007).
74 The summer of 2012 had the most extensive and long lasting melt event, with the greatest
75 observed runoff and net ice mass loss since satellite recordings began in 1979 (Tedesco *et al.*,
76 2013).

77 Subglacial environments contain active microbial communities (Sharp *et al.*, 1999;
78 Skidmore *et al.*, 2000; Yde *et al.*, 2010; Stibal *et al.*, 2012b; Dierer *et al.*, 2014) which
79 mediate chemical weathering (Wadham *et al.*, 2010, 2013; Montross *et al.*, 2013), resulting in
80 the release of solutes and nutrients to subglacial meltwater flows (Tranter *et al.*, 2005;
81 Wadham *et al.*, 2010, 2013; Montross *et al.*, 2013; Hawkings *et al.*, 2015). Bacterial
82 community profiles sampled from waters that emanate from beneath Russell Glacier, an outlet
83 glacier southwest of the GrIS, are distinct from nearby supraglacial waters, indicating that
84 microbial communities specific to subglacial environments are released from beneath the ice
85 sheet (Dierer *et al.*, 2014). While recent studies have reported the microbial abundance of
86 GrIS supraglacial snow and ice samples to range from $\sim 10^2$ to 10^6 cells ml⁻¹ (Cameron *et al.*,
87 2015; Stibal *et al.*, 2015a), and subglacial basal ice samples to have $\sim 9 \times 10^5$ cells g⁻¹ (Stibal
88 *et al.*, 2012a), there are currently no estimates for the magnitude of cells exported from glacial
89 environments during the melt season. Microbes transported from glaciers have the potential to
90 influence estuary ecosystems through the import of environmentally suited cells, which may
91 alter nutrient cycles and community composition (Garneau *et al.*, 2006, Gutiérrez *et al.*,
92 2015). The quantification and description of exported cells is therefore necessary to discern
93 what role they might play in downstream habitats.

94 Here we characterize and quantify microbial cells within meltwater samples from two
95 sites separated by ~ 30 km along the Watson River in southwest Greenland over the 2012 melt
96 season (Fig. 1). Water was captured at the first site as it exited the southwest of the GrIS, near

97 the Leverett Glacier outlet. Water was also collected at a second downstream site, fed by four
98 glacier outlets, prior to entering the river delta of the Søndre Strømfjord. To evaluate spatial
99 and temporal patterns in the microbial assemblages, we monitored and compared cell
100 concentrations and community structures at both sites using quantitative PCR (qPCR) and
101 16S rRNA gene sequencing approaches, and used multivariate analyses to identify factors
102 associated with the presence and diversity of the exported microbes. To reduce qPCR analysis
103 biases associated with gene copy quantification from DNA extracts of sediment-laden waters
104 (Stibal *et al.*, 2015a), qPCR standards were generated using DNA extracts from artificial river
105 water samples spiked with prokaryotic cultures, and using copy number per cell conversion
106 factors that were tailored to the amplicon diversity of each sample. Microbial cell export was
107 quantified by combining cell abundance with parallel hydrological records (discharge and
108 suspended sediment). Lastly, the nutritional significance of these river-transported microbiota
109 is considered using upscaling to estimate the magnitude of microbial release across the entire
110 GrIS.

111

112 **Results:**

113 *Discharge rates, sediment loads and chemistry:*

114 Mean daily discharge at KRS ranged from ca $80 \text{ m}^3 \text{ s}^{-1}$, at the start and end of the sample
115 period, to ca $2800 \text{ m}^3 \text{ s}^{-1}$, with two distinct peaks; one in early-mid July (DOY; 190-198), and
116 one late-July to early-August (DOY; 211-221, Fig. 2a). The mean annual volume of water
117 passing KRS from 2007 - 2013 was $\sim 4.44 \pm 2.28 \text{ km}^3$. Mean KRS daily sediment load was <
118 1.5 g L^{-1} before May 29 (DOY; 150) and after September 7 (DOY; 251), and fluctuated
119 between 1.44 g L^{-1} and 4.73 g L^{-1} between these dates (Fig. 2a). DOC values are reported in
120 Table S2.

121

122 *Cell abundance:*

123 Cell abundance, determined by qPCR analysis, was calculated to be between 9.48×10^3 cells
124 ml^{-1} to 7.44×10^5 cells ml^{-1} for all samples (Fig. 2b; mean abundance $1.15 \times 10^5 \pm 1.38 \times 10^5$
125 cells ml^{-1}). Differences between mean cell abundances calculated from LRS and KRS across
126 the sampling season were not found to be significantly different using a two-tailed *t*-test (LRS
127 mean; $8.30 \times 10^4 \pm 9.88 \times 10^4$ cells ml^{-1} , KRS mean; $1.50 \times 10^5 \pm 1.65 \times 10^5$ cells ml^{-1} , *t* =
128 1.30, *p* = 0.21). When a two-tailed paired *t*-test was performed using mean values from
129 pairwise dates (*n* = 7), no statistically significant difference was found (*t* = 0.71, *p* = 0.51). No
130 significant correlation was found between cell abundance at LRS or KRS when calculated
131 against discharge rates or sediment loads, with all Pearson's coefficient *r* values being $< \pm$
132 0.55 and all *p* values being > 0.16 . The mean abundance of archaea within LRS and KRS
133 samples was $2.91 \times 10^3 \pm 2.19 \times 10^3$ cells ml^{-1} and $2.65 \times 10^3 \pm 2.52 \times 10^2$ cells ml^{-1} ,
134 respectively, based on qPCR analysis using archaea specific primers. No correlation was
135 found between the abundance of archaea and discharge rates when a Pearson's correlation
136 analysis was performed (*r* = -0.21, *p* = 0.14).

137

138 *Amplicon sequencing read output:*

139 After sequence processing, the total number of reads generated from all samples was 889,724,
140 with an average of $17,795 \pm 4678$ reads per sample. Sequences were rarefied to 8670
141 sequences per sample, which resulted in the omission of a LRS June 3 replicate. After
142 rarefaction the mean number of OTU clusters per sample was 621.59 ± 225.29 . The
143 difference between the mean CatchAll calculated alpha diversity of the rarefied datasets was
144 not significant when calculated using a two-tailed Mann-Whitney U test (mean LRS CatchAll
145 calculated alpha diversity; 990.99 ± 331.04 , mean KRS CatchAll calculated alpha diversity;
146 1404.53 ± 668.70 , *Z*-score = -1.91, *p* = 0.06).

147

148 *Community composition:*

149 KRS and LRS rarefied communities consisted of OTU that were most closely related to
150 sequences belonging to 47 different phylum-level classifications. The majority of amplicons
151 were most closely related to six phylum level classifications; Proteobacteria ($65.33 \pm 4.85\%$;
152 $6.95 \times 10^4 \pm 8.44 \times 10^4$ cells ml^{-1}), Bacteroidetes ($20.66 \pm 4.36\%$; $3.53 \times 10^4 \pm 3.88 \times 10^4$ cells
153 ml^{-1}), Actinobacteria ($6.49 \pm 2.22\%$; $5.44 \times 10^3 \pm 9.08 \times 10^3$ cells ml^{-1}), Verrucomicrobia
154 ($1.75 \pm 1.11\%$; $1.06 \times 10^3 \pm 1.42 \times 10^3$ cells ml^{-1}), Chloroflexi ($1.16 \pm 0.69\%$; $9.34 \times 10^2 \pm$
155 1.36×10^3 cells ml^{-1}) and Acidobacteria ($1.08 \pm 0.58\%$; $6.65 \times 10^2 \pm 9.74 \times 10^2$ cells ml^{-1} ; Fig.
156 3a and b). The remaining 41 phylum-level classifications each had a mean amplicon relative
157 abundance of $< 1\%$. At the order level, the most dominant OTU were most closely related to
158 Burkholderiales ($32.76 \pm 9.31\%$; $2.90 \times 10^4 \pm 3.44 \times 10^4$ cells ml^{-1}), Flavobacteriales ($13.41 \pm$
159 6.78% ; $2.47 \times 10^4 \pm 2.90 \times 10^4$ cells ml^{-1}) and Methylophilales ($12.90 \pm 4.74\%$; $1.98 \times 10^4 \pm$
160 2.22×10^4 cells ml^{-1} ; Fig. 3c and d), and OTU relating to a further 234 order level
161 classifications were identified. Cyanobacteria related sequences, a potential proxy for
162 supraglacial water inputs, comprised $0.16 \pm 0.12\%$ ($2.04 \times 10^2 \pm 3.76 \times 10^2$ cells ml^{-1}) in each
163 community, and no relationship was found between discharge and their abundance when a
164 Pearson's correlation analysis was performed ($r = -0.22$, $p = 0.12$). The domain Archaea
165 constituted $0.18 \pm 0.10\%$ and $0.23 \pm 0.14\%$ of the total LRS and KRS prokaryotic amplicon
166 communities. Archaea related amplicons were predominantly most closely related to
167 Euryarchaeota ($0.06 \pm 0.05\%$) and Crenarchaeota ($0.05 \pm 0.04\%$).

168

169 *Factors contributing to community variability:*

170 Two-way crossed ANOSIM analysis of amplicon communities grouped by location and by
171 closest sampling date found them to be highly similar (location grouped $GlobalR = 0.934$, $p =$

172 0.001, date grouped *GlobalR*; 0.997 $p = 0.001$). Principal component analysis (PCA)
173 identified that 65% of variance in microbial community structure was explained within the
174 first 4 axes. To identify the most significant factors influencing microbial community
175 structure, a redundancy analysis (RDA) was performed with discharge, DOY, location (LRS
176 vs. KRS) and mean daily sediment load as the explanatory variables. These variables were
177 found to account for 40.2% of variance, with discharge accounting for the largest contribution
178 (22.3% of variance explained, $pseudoF = 13.5$, $p = 0.0025$), followed by DOY (10.7%,
179 $pseudoF = 7.3$, $p = 0.0025$) and location (4.8%, $pseudoF = 3.4$, $p = 0.0063$).

180 Mean daily sediment load was found to be insignificant in this analysis ($p = 0.068$). A
181 subset of data from LRS was also analysed from when water chemistry data were available
182 (DOY 144-207; see Table S2, S3 and S4). PCA explained 74.2% of total variance in the data
183 within the first 4 axes. When constrained by DOY, discharge, mean daily sediment load and
184 water chemistry, redundancy analysis explained 73.4% of variance within the first 4 axes.
185 Interactive forward selection identified the most significant factors, including discharge, pH
186 and nitrate concentration (each of them individually explaining 33% of variance at $p = 0.002$),
187 to be highly collinear. Mean daily sediment load and DOY were also found significant in the
188 analyses ($p < 0.001$), however, the robustness of this analysis should be taken with caution
189 due to the low number of samples and high number of predictors.

190 One-way ANOSIM analysis of communities from LRS and the secondary site, LRSc,
191 found them to be highly similar ($GlobalR = 0.987$, $p = 0.001$).

192

193 **Discussion:**

194 The abundance of cells within meltwater exiting Leverett Glacier and sampled at the LRS site
195 was stable throughout the study period, indicating that GrIS biomass release scales with
196 meltwater discharge. From this, it follows that fluxes of GrIS-derived biomass will increase

197 alongside climate-influenced elevated melt rates in the future (Mernild *et al.*, 2010; Fettweis
198 *et al.*, 2012), similar to dissolved and particulate material release (Hudson *et al.*, 2014;
199 Hawkings *et al.*, 2015). Community composition at the OTU level and mean cell
200 concentrations calculated downstream at KRS were found to be statistically similar to those at
201 LRS, despite almost 30 km of river length between sites and the inclusion of water from both
202 of the Watson River tributaries at the KRS site. This result suggests that terrestrial microbial
203 inputs were minimal, and that the neighbouring Ørkendalen and Isorlersuup glaciers to the
204 south of Leverett Glacier are releasing similar microbial assemblages in similar discharge-
205 influenced cell concentrations. This study therefore indicates that the glacial environment is
206 the predominant source of biomass transported downstream to the Søndre Strømfjord delta,
207 and in this respect, we can view the Watson River drainage system as a conceptual “pipe”
208 connecting the glacial environment, and its associated microbes, to the estuary. This model
209 contrasts to previous studies that have found downstream river communities to be seeded by
210 adjacent soils (Crump *et al.*, 2012), modified by flowing through lentic environments (Crump
211 *et al.*, 2007; Adams *et al.*, 2014), and varying with catchment area (Savio *et al.*, 2015). In the
212 case of the sampled Watson River, voluminous glacial melt may markedly dilute smaller
213 riparian and lake signal inputs, and bedrock substrata may limit hyporheic exchange.
214 Furthermore, we estimate that the river transit time between LRS and KRS sample points was
215 2.7 - 8.1 hours, using estimates of Watson River flow rates ($1 - 3 \text{ m s}^{-1}$), which is substantially
216 shorted than the multi-day residence time of water traveling through lentic environments
217 (Crump *et al.*, 2007; Adams *et al.*, 2014); equating to a reduced microbial water residence
218 time during which prokaryotic community compositions can develop, independent of input
219 sources (Adams *et al.*, 2014).

220 Data pertaining to cell concentrations in GrIS glacial meltwaters are currently
221 unreported, however, prokaryotic cells were found to be an order of magnitude more

222 concentrated within LRS samples than within surface ice meltwater samples analysed from
223 Russell Glacier in 2012 ($8.38 \times 10^3 \pm 9.85 \times 10^3$ cells ml⁻¹ calculated from 13 samples
224 collected between 7 June and 25 August; Cameron and Junge; unpublished). When compared
225 to surface ice meltwaters from Midre Lovénbreen glacier in Svalbard, waters at LRS were
226 found to be four fold more concentrated than combined bacterial, archaeal and eukaryotic cell
227 concentrations reported by Irvine-Fynn *et al.* (2012; $\sim 2 \times 10^4$ cells ml⁻¹), and two to four fold
228 higher than concentrations reported by Mindl *et al.* (2007; 1.38×10^4 to 4.84×10^4 cells ml⁻¹).
229 Prokaryotic cells sampled from LRS and KRS were an order of magnitude less abundant than
230 the bacterioplankton sampled from river and estuary waters of the Lena River, the second
231 largest Arctic Ocean river input ($>1.5 \times 10^6$ cells ml⁻¹; Sorokin & Sorokin, 1996; Dittmar &
232 Kattner, 2003), and were of similar abundance to waters sampled from Mackenzie River, the
233 fourth largest Arctic Ocean river input (6.3×10^5 cells ml⁻¹; Garneau *et al.*, 2006; Dittmar &
234 Kattner, 2003), and a Patagonian glacial-fed fjord ($\sim 10^5$ cells ml⁻¹; Gutiérrez *et al.*, 2015).
235 Given the size of the Lena and Mackenzie river catchment areas (2.4×10^6 km² and 1.8×10^6
236 km² respectively; Holmes *et al.*, 2000; Emmerton *et al.*, 2008), the variety of landscapes
237 through which they flow, and the rich marine and terrestrial biotic and nutritional inputs that
238 Patagonian fjord waters receive, the comparable cell abundance of these systems to LRS and
239 KRS waters highlights the notable concentrations of biota that are exported from the GrIS
240 during the melt season. Our study was coincidentally performed during the highest discharge
241 year since records began in 1979 (Tedesco *et al.*, 2013), however, most of this melt event was
242 captured during two distinct peaks, which were not sampled in this study (Fig. 2a), and we
243 therefore believe our reported concentrations to be representative estimates. We however note
244 that beyond the filtration of samples through 0.22 μ m polyethersulfone filters (Liang and
245 Keeley, 2013), no steps were taken to further reduce or quantify the amplification of

246 extracellular DNA (e.g Nielsen et al., 2007, Kim et al., 2016), therefore our values may
247 overestimate abundance.

248 LRS and KRS communities were diverse and dominated by Proteobacteria,
249 Bacteroidetes and Actinobacteria. Like the subglacial outflow waters of Russell Glacier
250 (Dieser *et al.*, 2014), samples from both sites were found to have high percentages of OTU
251 that were most closely related to Burkholderiales, and OTU related to Actinomycetales,
252 Flavobacteriales, Methylococcales and Methylophilales were all found to have relative
253 abundances of >1% in both studies. Likewise, OTU related to orders Burkholderiales and
254 Gallionellales, which contain a high numbers of iron-oxidizing chemolithotrophic bacteria,
255 were found to be predominant within these samples (Fig. 3) and within samples taken from
256 the subglacial environment of Robertson Glacier, Canada (Hamilton *et al.*, 2013).

257 Cyanobacteria comprised ~0.2% of samples from both sites, similar to previous
258 reports of subglacial environments (Hamilton *et al.*, 2013; Dieser *et al.*, 2014). Since
259 Cyanobacteria typically dominate surface ice and associated debris (with up to ~80% relative
260 abundance, Stibal *et al.*, 2015b; Cameron *et al.*, 2016), this result suggests that the majority of
261 biomass within this study originated from the subglacial environment. In contrast, a study
262 from a small subglacial outflow of Russell Glacier found that only 21% of sequences were
263 unique to its subglacial environment (Dieser *et al.*, 2014), while 76% were common to both
264 supra- and subglacial libraries. While the subglacial drainage network of Leverett Glacier is
265 likely substantially more extensive than that of Russell Glacier, leading to a greater subglacial
266 signal in meltwater, caution should nevertheless be taken when using biotic signatures to
267 determine the origins of microbial material.

268 Of the minimal dissimilarities found between the temporally sampled microbial
269 assemblages, discharge explained between 20-30% of variance, with sample date also being
270 significant. This is likely to be the result of a seasonally-developing subglacial drainage

271 system (Bartholomew *et al.*, 2011; Chandler *et al.*, 2013), facilitating the release of different
272 reserves of subglacial microbiota as the area of subglacial drainage expands further from the
273 margin. Changes in the proportion of supraglacial to subglacial source water may also
274 contribute to the variance in the community structure data; however, the lack of correlation
275 between discharge and the relative abundance of Cyanobacteria does not corroborate this
276 explanation. One way that supra- and subglacial contributions could be discerned is by
277 sampling during “outburst events”, which are discreet periods of subglacial flushing that
278 occur several times per melt season (Hawkings *et al.*, 2014). As our sampling regime was not
279 explicitly designed to test this, outburst peaks were not captured in this study (although
280 sample DOY 177 may be on the rising limb of the first outburst, Fig. 2a). Sampling outburst
281 events may offer future insight into the composition and ecology of subglacial microbial
282 communities, and may shed additional light onto potential estuarine contributions.

283 Over the course of the 2012 melt season, we estimate that a total volume of $\sim 6.83 \text{ km}^3$
284 of water passed the KRS sample site. The mean cell abundance at KRS was calculated to be
285 $1.50 \times 10^5 \text{ cells ml}^{-1}$, which equates to $\sim 1.02 \times 10^{21}$ cells, or $\sim 30.95 \text{ Mg}$ of cell associated
286 carbon, $\sim 5.94 \text{ Mg}$ of cell associated nitrogen, and $\sim 1.54 \text{ Mg}$ of cell associated phosphorus
287 flowing into the fjord (based on mean cellular carbon and nitrogen contents of surface coastal
288 bacterial assemblages; $30.2 \text{ fg C cell}^{-1}$ and $5.8 \text{ fg N cell}^{-1}$ respectively; Fukuda *et al.*, 1998,
289 and a P:C ratio of 0.05; Fagerbakke *et al.*, 1996, Table 1). Based on mean early- to mid-melt
290 season DOC ($0.26 \mu\text{g ml}^{-1}$), and mean 2009 and 2010 particulate organic carbon
291 concentrations from Leverett Glacier ($2.33 \mu\text{g ml}^{-1}$; Lawson *et al.*, 2014b), we estimate that a
292 total of $\sim 17.68 \times 10^3 \text{ Mg}$ of organic carbon flowed into the fjord during the 2012 melt season,
293 and that cell biomass contributed towards $\sim 0.18\%$ of this (Table 1). Estimates of total organic
294 nitrogen flux to the fjord were calculated to be $1.02 \times 10^3 \text{ Mg}$, using mean dissolved organic
295 nitrogen concentrations ($0.026 \mu\text{g ml}^{-1}$; Wadham *et al.*, submitted) and estimates of particulate

296 nitrogen from Leverett Glacier outflow water sampled in 2015 ($0.12 \mu\text{g ml}^{-1}$; Kohler, Zarsky,
297 Stibal *et al.*, unpublished). We estimate that cells account for $\sim 1.40\%$ of the total organic
298 nitrogen that flowed to the fjord. Mean total organic phosphorus concentrations were
299 calculated to be $0.03 \mu\text{g ml}^{-1}$ (dissolved organic phosphorus; DOP; $0.001 \mu\text{g ml}^{-1}$; Hawkings
300 *et al.*, 2016, particulate organic phosphorus; $0.03 \mu\text{g ml}^{-1}$), amassing to $\sim 225.49 \text{ Mg}$ of
301 organic P flowing into the fjord, of which we estimate that 0.68% originates from biomass
302 (Table 1). Estimates of the percentage contribution of cells to organic C and N fluxes at KRS
303 were approximately half of those calculated from the four largest Arctic Ocean river inputs
304 (Yenisey, Lena, Ob and Mackenzie rivers, termed “Big-4 Arctic rivers” herein; Table 1).
305 Estimated KRS cellular contributions to DOP was three fold higher than the Big-4 Arctic
306 rivers calculated cellular percentage contribution, however it should be noted that there was
307 an order of magnitude difference between DOP concentrations calculated from Lena River
308 (Dittmar & Kattner, 2003) and Mackenzie River (Emmertson *et al.*, 2008) sampled waters. As
309 far as the authors are aware, the particulate organic phosphorus fraction of the Lena and
310 Mackenzie River systems is unreported so cellular contribution to TOP cannot be commented
311 on.

312 The mean freshwater runoff across the whole of the GrIS was estimated to be $419.34 \pm$
313 $54.22 \text{ km}^3 \text{ yr}^{-1}$ between 2000 and 2006 (Fettweis, 2007). Assuming that glacial discharge cell
314 concentrations are homogenous across the GrIS, and that they are stable between melt years,
315 based on cell abundance at KRS we calculate that $\sim 6.29 \times 10^{22} \text{ cells yr}^{-1}$ are transported from
316 the ice sheet to surrounding environments, equating to $\sim 1900 \text{ Mg yr}^{-1}$ of cell associated
317 carbon, $\sim 365 \text{ Mg yr}^{-1}$ of cell associated nitrogen, and $\sim 95 \text{ Mg yr}^{-1}$ of cell associated
318 phosphorus. This cell flux was at least seventeen times lower than the combined estimated
319 flux from the Big-4 Arctic rivers, which individually have similar annual discharge rates to
320 the estimated annual GrIS freshwater runoff (discharge rates range from $249 - 333 \text{ km}^3 \text{ yr}^{-1}$,

321 Mackenzie River, to 562 - 577 km³ yr⁻¹, Yenisey River; Dittmar & Kattner, 2003). The
322 estimated C, N and P nutrient contributions to downstream environments is an order of
323 magnitude lower than exports from the Big-4 Arctic rivers (Table 1). However, while cells
324 within Arctic glacier and ice sheet-fed rivers systems are found to contribute minimally
325 towards nutrient budgets, we argue that the focus of their importance lies within the ability of
326 viable and environmentally suited microorganisms, regardless of their abundance (Wilhelm et
327 al., 2014), to recycle organic nutrients within downstream fjord, estuary and delta
328 environments. Our estimates of cell export from the GrIS were calculated using mean
329 freshwater runoff values and prokaryotic abundance estimates from four glacial outlets in
330 southwest Greenland. These estimates neither account for cell loss or freshwater flux from
331 solid ice discharge or tundra runoff, which together amount to approximately two thirds of the
332 freshwater flux from Greenland (Bamber *et al.*, 2012), nor do they consider the transportation
333 of eukaryotes from the glacial environment. Supraglacial communities have been found to
334 vary spatially across the GrIS (Cameron *et al.*, 2016), and we therefore envisage that
335 subglacial GrIS communities will similarly vary spatially as a result of changing
336 environmental conditions such as bedrock geology and nutrient availability, as has been
337 considered in subglacial systems previously (Stibal *et al.*, 2012a). We therefore consider that
338 our estimates of cells release are conservative and oversimplified, however they nonetheless
339 provide a valuable first insight into the potential biological significance of the GrIS to
340 downstream environments.

341 In summary, bacteria and archaea were exported from Leverett Glacier, an outlet of
342 the Greenland Ice Sheet, in the order of 8.30×10^4 cells ml⁻¹, with Proteobacteria,
343 Bacteroidetes and Actinobacteria dominating these microbial assemblages. We propose that
344 the subglacial environment is the primary source of biomatter that passes LRS and KRS
345 sample sites. Since biomass release scales with discharge, we hypothesise that as meltwater

346 from the GrIS increases in a warming world, so too will the displacement of subglacial biota
347 to surrounding ecosystems. The role that these microbes play in estuaries is at present poorly
348 described, therefore investigation into how these communities are assembled is timely during
349 this current period of deglaciation.

350

351 **Experimental Procedures:**

352 *Study sites*

353 The Watson River overrides Archaen gneiss and granite (Henriksen *et al.*, 2009) and is made
354 up of two main tributaries that drain four major lobes of the GrIS in southwestern Greenland,
355 including, from north to south, Russell, Leverett, Ørkendalen and Isorlersuup glaciers (Fig. 1).
356 Leverett Glacier has a hydrologically active drainage area of ~600 km² (Cowton *et al.*, 2012).
357 Russell and Leverett glacial melt rivers combine to form the Akuliarusiarsuup Kuua, which
358 flows through the Sandflugtsdalen valley and serves as the northern tributary to the Watson
359 River, which discharges into the Søndre Strømfjord. The southern tributary, Qinnguata
360 Kuussua, flows through the Ørkendalen valley and drains the Ørkendalen and Isorlersuup
361 glaciers (Lindbäck *et al.*, 2014) before converging with the Akuliarusiarsuup Kuua upstream
362 of Kangerlussuaq. The Qinnguata Kuussua is broader than the Akuliarusiarsuup Kuua, and
363 several proglacial lakes are present. Due to difficulty in accessing the Qinnguata Kuussua it
364 was not possible to monitor this tributary.

365 Sampling and measurements were undertaken between 10 May and 26 September
366 2012 (Table S1), encompassing the record breaking melt year (Tedesco *et al.*, 2013). Two
367 sampling sites were selected in order to distinguish between material immediately exiting the
368 GrIS and upon entering the fjord. The inland Leverett River site (LRS; 67° 3.92'N, 50°
369 9.91'W) captured the subglacial outflow waters from Leverett Glacier. Due to anomalously
370 high waters making LRS inaccessible, an alternative site (LRSc; 67° 4.25'N, 50° 17.17'W) ca

371 5 km downstream at the confluence of Leverett and Russell glacial outflow rivers was used
372 from 16 August onwards (three sampling events, Table S1; Fig. 1). The abbreviation LRS is
373 used to refer to both sites, unless otherwise stated herein. The downstream Kangerlussuaq
374 river site (KRS; 67° 0.30'N, 50° 41.18'W) was situated ca 27 km downstream along the
375 Akuliarusiarsuup Kuua, below the convergence with the Qinnguata Kuusua, and immediately
376 before the Watson River empties into the delta at the head of the Søndre Strømfjord (Fig. 1).

377

378 *Discharge, sediment load and chemistry*

379 The methods used for measuring and calculating discharge and sediment load at KRS are
380 described in Hasholt *et al.* (2012). Discharge and sediment load were collected from 2007
381 until 2013. Chemical analyses of the sampled waters have been reported previously
382 (Hawkings *et al.*, 2014, 2015, 2016; Wadham *et al.*, submitted) and are summarized with
383 permission in Tables S2, S3 and S4. Mean particulate organic P was calculated from 6 LRS
384 samples taken on day of year 2012 (DOY) 131, 145, 168, 177, 184 and 207 (Hawkings *et al.*,
385 2016). Data for dissolved organic carbon (DOC) were determined by high temperature
386 combustion catalytic oxidation (680 °C) using a Shimadzu TOC-V analyser (Kyoto, Japan)
387 with a high sensitivity catalyst, as described by Lawson *et al.* (2014b). Precision and accuracy
388 were $< \pm 7 \%$ and the limit of detection was $< 1 \mu\text{M}$.

389

390 *Microbiology*

391 For microbiological analyses, triplicate river water samples were collected into sterile 50 ml
392 syringes and were immediately filtered through Sterivex-GP 0.22 μm polyethersulfone filters
393 (Millipore, Billerica, MA, USA) until the filter clogged (35 - 175 ml depending on the
394 suspended sediment content; volumes filtered per date and location are shown in Table S1).
395 Liquid was expelled from the filters, filter inlets and outlets were closed using sterile caps,

396 and filter units were stored at -20°C within 20 minutes from collection, or were stored next to
397 frozen icepacks for up to two hours prior to storage at -20°C. Samples were transported frozen
398 to home laboratories in Copenhagen.

399 DNA extraction from filtered samples was performed no later than two weeks after
400 collection. The filters were thawed at room temperature in a sterile laminar flow cabinet and
401 DNA was extracted using the PowerWater Sterivex DNA Isolation Kit (MO BIO
402 Laboratories, Carlsbad, CA, USA) following the manufacturer's protocol. An unused Sterivex
403 filter was extracted alongside each batch of extractions as a procedural control. These
404 procedural controls were processed for sequence library preparation until the point of
405 quantification.

406 Prokaryotic 16S rRNA genes from river sample DNA extracts were quantified,
407 relative to the DNA extracts of artificial river water standards, by using a qPCR set-up with
408 primer pairs 341F (5'-CCTACGGGAGGCAGCAG-3') and 518R (5'-
409 ATTACCGCGGCTGCTGG-3'; Muyzer *et al.*, 1993) to target prokaryotic 16S rRNA genes,
410 and 931F (5'-AGGAATTGGCGGGGAGCA-3'; Jackson *et al.*, 2001) and 1100R (5'-
411 BGGGTCTCGCTCGTTRCC-3'; Einen *et al.*, 2008) to target archaeal 16S rRNA genes. Cell
412 abundance data was generated using qPCR analyses in combination with the mean 16S rRNA
413 gene copy number per cell for each sample, based on reference Greengenes OTU 16S rRNA
414 gene copy numbers per cell (Langille *et al.*, 2013). The mean 16S rRNA gene copy number
415 per cell of the standard inoculant mix was 2.18 ± 0.40 copies cell⁻¹ for prokaryotes and $3.00 \pm$
416 0.00 copies cell⁻¹ for archaea. The mean 16S rRNA gene copy number per cell of the
417 samples was 2.98 ± 0.23 copies cell⁻¹ for prokaryotes and 1.83 ± 0.47 copies cell⁻¹ for
418 archaea based on non-rarefied amplicon diversity. Reaction mixtures (20 µl total) consisted of
419 1 µl of template DNA, 10 µl of SYBR Premix DimerEraser (TaKaRa, Japan) and 0.8 µl of the
420 forward and reverse primers (10 pmol µl⁻¹). The cycle program was 95 °C for 30 s followed

421 by 50 cycles of 95 °C for 30 s, 55 °C for 30 s for primer pair 341F-518R, or 64 °C for 30 s for
422 primer pair 931F-1100R, and 72 °C for 30 s. The reaction was completed by a final 72 °C
423 elongation step for 6 min and followed by high-resolution melt curve analysis in 0.5 °C
424 increments from 55 to 98 °C. The abundance of bacteria and archaea in the samples was
425 determined using qPCR on a CFX96 Touch real-time PCR detection system (Bio-Rad, CA,
426 USA). All qPCR reactions were performed in duplicate and were prepared under DNA free
427 conditions in a pressurized clean-lab with a HEPA filtered air inlet and nightly UV-
428 irradiation. Beyond the filtration of samples through Sterivex-GP 0.22 µm polyethersulfone
429 filters, no further steps were taken to prevent or quantify the amplification of extracellular
430 DNA. In order to achieve accurate cell abundance quantification unbiased by DNA extraction,
431 procedural qPCR standards were prepared. Heat-sterilised (450 °C for 8 hours) river
432 sediment from the Watson River delta was re-suspended in autoclaved deionised water using
433 a ratio of 2 g sediment per litre in order to simulate the natural river sediment load. Cultures
434 of the aerobic heterotroph *Variovorax paradoxus* (Betaproteobacteria), methanotroph
435 *Methylosinus sporium* (Alphaproteobacteria) and methanogen *Methanosphaerula palustris*
436 (Euryarchaeota), representing typical components of a subglacial community (Stibal *et al.*,
437 2012), were counted using epifluorescence microscopy and then immediately added to the
438 sediment suspension in a 9:1:1 ratio to obtain a final concentration of 1.1×10^9 cells g⁻¹
439 sediment. Serial dilutions (1:10) of the artificial river water were prepared to generate five
440 further concentrations, down to 1.1×10^4 cells g⁻¹ sediment. A blank standard containing no
441 cells was also included. Each procedural standard (60 ml) was filtered through a Sterivex
442 filter. Filters were then sealed with sterile caps and frozen at -20 °C for at least 24 hours,
443 before DNA was extracted from them following the same protocol as for the samples.
444 Sequence library preparation from DNA extracts, sequencing and downstream quality
445 filtering and analysis was performed as described in Cameron *et al.*, 2016, with the exception

446 that samples were rarefied to 8670 sequences per sample. This protocol has been included as
447 supplementary information. All negative and procedural controls that were processed for
448 sequence library preparation had a final DNA concentration of $\leq 0.8 \text{ ng ml}^{-1}$, therefore these
449 amplicons were not sequenced. Operational taxonomic units (OTU) were defined as
450 sequences that possessed $\geq 97\%$ identity. Amplicon data are available at The European
451 Bioinformatics Institute under study accession number PRJEB12394. (<http://www.ebi.ac.uk>).

452

453 *Statistical analyses*

454 CatchAll (Bunge, 2011) was used to calculate parametric alpha diversity. Untransformed
455 Bray–Curtis resemblance and analysis of similarity (ANOSIM) were calculated from OTU
456 matrices using PRIMER-E version 6 (Plymouth, UK). Multivariate statistical analysis was
457 used to explain the variation in the community composition data as a function of sample
458 location and environmental variables. The relative abundance data were $\arcsin\sqrt{x}$ transformed
459 prior to analysis. All data were standardised and centred. Detrended canonical correspondence
460 analysis (DCCA) was used to determine the length of the gradient along the first ordination
461 axis in order to select the appropriate method for ordination of the data. A combination of
462 unconstrained and constrained analysis was used to explain the variation in the data.

463 Interactive forward selection with 999 Monte Carlo permutations was used in the constrained
464 analysis. The p values were corrected for multiple testing using false discovery rate. All
465 multivariate data analyses were performed using the software Canoco 5 (Microcomputer
466 Power, NY, USA).

467

468 **Acknowledgements:**

469 This research was funded by Danish Research Council grants FNU 10-085274 to CJ and
470 CENPERM DNRF100. It has additionally been supported by a NERC grant NE/I008845/1 to

471 JLW, and by a Czech Science Foundation grant GACR 15-17346Y to MS. We thank Pernille
472 Stockmarr for technical assistance.

473

474 The authors declare that there are no conflicts of interest.

475

476 **References:**

477 Adams, H.E., Crump, B.C., and Kling, G.W. (2014) Metacommunity dynamics of bacteria in
478 an arctic lake: the impact of species sorting and mass effects on bacterial production and
479 biogeography. *Front Microbiol* 5: 82.

480 Bamber, J., Van Den Broeke, M., Ettema, J., Lenaerts, J., and Rignot, E. (2012) Recent large
481 increases in freshwater fluxes from Greenland into the North Atlantic. *Geophys Res Lett* 39:
482 L19501.

483 Bartholomew, I., Nienow, P., Sole, A., Mair, D., Cowton, T., Palmer, S., and Wadham, J.
484 (2011) Supraglacial forcing of subglacial drainage in the ablation zone of the Greenland ice
485 sheet. *Geophys Res Lett* 38: L08502.

486 Bhatia, M.P., Kujawinski, E.B., Das, S.B., Breier, C.F., Henderson, P.B., and Charette, M.A.
487 (2013) Greenland meltwater as a significant and potentially bioavailable source of iron to the
488 ocean. *Nat Geosci* 6: 274-278.

489 Bunge, J. (2011) Estimating the number of species with CatchAll. *Biocomputing* 121–30.

490 Cameron, K.A., Hagedorn, B., Diesler, M., Christner, B.C., Choquette, K., Sletten, R., *et al.*
491 (2015) Diversity and potential sources of microbiota associated with snow on western
492 portions of the Greenland Ice Sheet. *Environ Microbiol* 17: 594-609.

- 493 Cameron, K.A., Stibal, M., Zarsky, J.D., Gözdereliler, E., Schostag, M., and Jacobsen, C.S.
494 (2016) Supraglacial bacterial community structures vary across the Greenland ice sheet.
495 FEMS Microbiol Ecol 92: fiv164.
- 496 Cauwet, G., and Sidorov, I. (1996) The biogeochemistry of Lena River: organic carbon and
497 nutrients distribution. Mar Chem 53: 211-227.
- 498 Chandler, D.M., Wadham, J.L., Lis, G.P., Cowton, T., Sole, A., Bartholomew, I., *et al.* (2013)
499 Evolution of the subglacial drainage system beneath the Greenland Ice Sheet revealed by
500 tracers. Nat Geosci 6: 195-198.
- 501 Clason, C.C., Mair, D.W.F., Nienow, P.W., Bartholomew, I.D., Sole, A., Palmer, S., and
502 Schwanghart, W. (2015) Modelling the transfer of supraglacial meltwater to the bed of
503 Leverett Glacier, southwest Greenland. Cryosphere 8: 123-138.
- 504 Comiso, J.C. (2006) Arctic warming signals from satellite observations. Weather 61: 70-76.
- 505 Cowton, T., Nienow, P., Bartholomew, I., Sole, A., and Mair, D. (2012) Rapid erosion
506 beneath the Greenland ice sheet. Geology 40: 343-346.
- 507 Crump, B.C., Adams, H.E., Hobbie, J.E., and Kling, G.W. (2007) Biogeography of
508 bacterioplankton in lakes and streams of an arctic tundra catchment. Ecology 88: 365-1378.
- 509 Crump, B.C., Amaral-Zettler, L.A., and Kling, G.W. (2012) Microbial diversity in arctic
510 freshwaters is structured by inoculation of microbes from soils. ISME J 6: 1629-1639.
- 511 Dieser, M., Broensen, E.L.J.E., Cameron, K.A., King, G.M., Achberger, A., Choquette, K., *et*
512 *al.* (2014) Molecular and biogeochemical evidence for methane cycling beneath the western
513 margin of the Greenland Ice Sheet. ISME J 8: 2305-2316.

- 514 Dittmar, T., and Kattner, G. (2003) The biogeochemistry of the river and shelf ecosystem of
515 the Arctic Ocean: a review. *Mar Chem* 83: 103-120.
- 516 Einen, J., Thorseth, I.H., and Øvreås, L. (2008) Enumeration of Archaea and Bacteria in
517 seafloor basalt using real-time quantitative PCR and fluorescence microscopy. *FEMS*
518 *Microbiol Lett* 282: 182-187.
- 519 Emmerton, C.A., Lesack, L.F.W., and Vincent, W.F. (2008) Nutrient and organic matter
520 patterns across the Mackenzie River, estuary and shelf during the seasonal recession of sea-
521 ice. *J Marine Syst* 74: 741-755.
- 522 Fagerbakke, K.M., Heldal, M., and Norland, S. (1996) Content of carbon, nitrogen, oxygen,
523 sulfur and phosphorus in native aquatic and cultured bacteria. *Aquat Microb Ecol* 10: 15-27.
- 524 Fettweis, X. (2007) Reconstruction of the 1979–2006 Greenland ice sheet surface mass
525 balance using the regional climate model MAR. *The Cryosphere Discussions* 1: 123-168.
- 526 Fettweis, X., Tedesco, M., Van Den Broeke, M., and Ettema, J. (2011) Melting trends over
527 the Greenland ice sheet (1958–2009) from spaceborne microwave data and regional climate
528 models. *Cryosphere* 5: 359-375.
- 529 Fettweis, X., Franco, B., Tedesco, M., Van Angelen, J.H., Lenaerts, J.T.M., Van Den Broeke,
530 M.R., and Gallée, H. (2012) Estimating Greenland ice sheet surface mass balance
531 contribution to future sea level rise using the regional atmospheric climate model MAR.
532 *Cryosphere* 7: 3101-3147.
- 533 Fukuda, R., Ogawa, H., Nagata, T., and Koike, I. (1998) Direct determination of carbon and
534 nitrogen contents of natural bacterial assemblages in marine environments. *Appl Environ*
535 *Microbiol* 64: 3352-3358.

- 536 Garneau, M-È., Vicent, W.F., Alonso-Sáez, L., Gratton, Y., and Lovejoy, C. (2006)
537 Prokaryotic community structure and heterotrophic production in a river-influenced coastal
538 Arctic ecosystem. *Aquat Microb Ecol* 42: 27-40.
- 539 Gutiérrez, M.H., Galand, P.E., Moffat, C., and Pantoja, S. (2015) Melting glacier impacts
540 community structure of Bacteria, Archaea and Fungi in a Chilean Patagonia fjord. *Environ*
541 *Microbiol* 17: 3882-3897.
- 542 Hallet, B., Hunter, L., and Bogen, J. (1996) Rates of erosion and sediment evacuation by
543 glaciers: A review of field data and their implications. *Glob Planet Change* 12: 213-235.
- 544 Hamilton, T.L., Peters, J.W., Skidmore, M.L., and Boyd, E.S. (2013) Molecular evidence for
545 an active endogenous microbiome beneath glacial ice. *ISME J* 7: 1402-1412.
- 546 Hanna, E., Huybrechts, P., Steffen, K., Cappelen, J., Huff, R., Shuman, C., *et al.* (2008)
547 Increased runoff from melt from the Greenland Ice Sheet: a response to global warming. *J*
548 *Climate* 21: 331-341.
- 549 Hasholt, B., Bobrovitskaya, N., Bogen, J., Mcnamara, J., Mernild, S.H., Milburn, D., and
550 Walling, D.E. (2006) Sediment transport to the Arctic Ocean and adjoining cold oceans.
551 *Hydrol Res* 37: 413-432.
- 552 Hasholt, B., Mikkelsen, A.B., Nielsen, M.H., and Larsen, M.A.D. (2012) Observations of
553 runoff and sediment and dissolved loads from the Greenland ice sheet at Kangerlussuaq, West
554 Greenland, 2007 to 2010. *Z Geomorphol, Supplementary Issue* 57: 3-27.
- 555 Hawkings, J.R., Wadham, J.L., Tranter, M., Raiswell, R., Benning, L.G., Statham, P.J., *et al.*
556 (2014) Ice sheets as a significant source of highly reactive nanoparticulate iron to the oceans.
557 *Nat Commun* 5: 3929.

- 558 Hawkings, J.R., Wadham, J., Tranter, M., Lawson, E., Sole, A., Cowton, T., *et al.* (2015) The
559 effect of warming climate on nutrient and solute export from the Greenland Ice Sheet.
560 *Geochem Perspect Lett* 1: 94-104.
- 561 Hawkings, J., Wadham, J., Tranter, M., Telling, J., Bagshaw, E., Beaton, A., *et al.* (2016) The
562 Greenland Ice Sheet as a hotspot of phosphorus weathering and export in the Arctic. *Glob*
563 *Biogeochem Cy* 30: 191-210.
- 564 Henriksen, N., Higgins, A.K., Kalsbeek, F., Pulvertaft, T., and Christopher, R. (2009)
565 Greenland from Archaean to Quaternary: descriptive text to the 1995 Geological map of
566 Greenland, 1: 2 500 000. Geological Survey of Denmark and Greenland Bulletin 18.
- 567 Holmes, R.M., Peterson, B.J., Gordeev, V.V., Zhulidov, A.V., Meybeck, M., Lammers, R.B.,
568 and Vörösmarty, C.J. (2000) Flux of nutrients from Russian rivers to the Arctic Ocean: Can
569 we establish a baseline against which to judge future changes? *Water Resour Res* 36: 2309-
570 2320.
- 571 Hudson, B., Overeem, I., McGrath, D., Syvitski, J.P.M., Mikkelsen, A., and Hasholt, B.
572 (2014) MODIS observed increase in duration and spatial extent of sediment plumes in
573 Greenland fjords. *Cryosphere* 8: 1161-1176.
- 574 Irvine-Fynn, T.D.L., Edwards, A., Newton, S., Langford, H., Rassner, S.M., Telling, J. *et al.*
575 (2012) Microbial cell budgets of an Arctic glacier surface quantified using flow cytometry.
576 *Environmental Microbiology* 14: 2998-3012.
- 577 Jackson, C.R., Langner, H.W., Donahoe, Christiansen, J., Inskeep, W.P., and McDermott,
578 T.R. (2001) Molecular analysis of microbial community structure in an arsenite-oxidizing
579 acidic thermal spring. *Environ Microbiol* 3: 532-542.

- 580 Kim, J.-H., Kim, J.H., Wang, P., Park, B.S., and Han, M.-S. (2016) An Improved Quantitative
581 Real-Time PCR Assay for the Enumeration of *Heterosigma akashiwo* (Raphidophyceae)
582 Cysts Using a DNA Debris Removal Method and a Cyst-Based Standard Curve. PLoS ONE
583 11: e0145712.
- 584 Langille, M.G.I., Zaneveld, J., Caporaso, J.G., McDonald, D., Knights, D., Reyes, J.A. et al.
585 (2013) Predictive functional profiling of microbial communities using 16S rRNA marker gene
586 sequences. Nat Biotech 31: 814-821.
- 587 Lawson, E.C., Bhatia, M.P., Wadham, J.L., and Kujawinski, E.B. (2014a) Continuous
588 summer export of nitrogen-rich organic matter from the Greenland Ice Sheet inferred by
589 ultrahigh resolution mass spectrometry. Environ Sci Technol 48: 14248-14257.
- 590 Lawson, E.C., Wadham, J.L., Tranter, M., Stibal, M., Lis, G.P., Butler, C.E.H., et al. (2014b)
591 Greenland Ice Sheet exports labile organic carbon to the Arctic oceans. Biogeosciences 11:
592 4015-4028.
- 593 Leeson, A.A., Shepherd, A., Briggs, K., Howat, I., Fettweis, X., Morlighem, M., and Rignot,
594 E. (2014) Supraglacial lakes on the Greenland ice sheet advance inland under warming
595 climate. Nat Clim Chang 5: 51-55.
- 596 Liang, Z., and Keeley, A. (2013) Filtration recovery of extracellular DNA from
597 environmental water samples. Environ Sci Technol 47: 9324-9331.
- 598 Lindbäck, K., Pettersson, R., Doyle, S.H., Helanow, C., Jansson, P., Kristensen, S.S., et al.
599 (2014) High-resolution ice thickness and bed topography of a land-terminating section of the
600 Greenland Ice Sheet. Earth Syst Sci Data 6: 331-338.

- 601 Mernild, S.H., Liston, G.E., Hiemstra, C.A., and Christensen, J.H. (2010) Greenland ice sheet
602 surface mass-balance modeling in a 131-yr perspective, 1950-2080. *J Hydrometeorol* 11: 3-
603 25.
- 604 Mindl, B., Anesio, A.M., Meirer, K., Hodson, A.J., Laybourn-Parry, J., Sommaruga, R., and
605 Sattler, B. (2007) Factors influencing bacterial dynamics along a transect from supraglacial
606 runoff to proglacial lakes of a high Arctic glacier. *FEMS Microbiol Ecol* 59: 307-317.
- 607 Montross, S.N., Skidmore, M., Tranter, M., Kivimäki, A-L., and Parkes, R.J. (2013) A
608 microbial driver of chemical weathering in glaciated systems. *Geology* 41: 215-218.
- 609 Muyzer, G., De Waal, E.C., and Uitterlinden, A.G. (1993) Profiling of complex microbial
610 populations by denaturing gradient gel electrophoresis analysis of polymerase chain reaction-
611 amplified genes coding for 16S rRNA. *Appl Environ Microbiol* 59: 695-700.
- 612 Nielsen, K.M., Johnsen, P.J., Bensasson, D., and Daffonchio, D. (2007) Release and
613 persistence of extracellular DNA in the environment. *Environmental biosafety research* 6: 37-
614 53.
- 615 Rignot, E., Velicogna, I., Van Den Broeke, M.R., Monaghan, A., and Lenaerts, J.T.M. (2011)
616 Acceleration of the contribution of the Greenland and Antarctic ice sheets to sea level rise.
617 *Geophys Res Lett* 38: L05503.
- 618 Savio, D., Sinclair, L., Ijaz, U.Z., Parajka, J., Reischer, G.H., Stadler, P., *et al.* (2015)
619 Bacterial diversity along a 2600 km river continuum. *Environ Microbiol* 17: 4994-5007.
- 620 Sharp, M., Parkes, J., Cragg, B., Fairchild, I.J., Lamb, H., and Tranter, M. (1999) Widespread
621 bacterial populations at glacier beds and their relationship to rock weathering and carbon
622 cycling. *Geology* 27: 107-110.

- 623 Shepherd, A., Ivins, E.R., A, G., Barletta, M.J., Bentley, M.J., Bettadpur, S., *et al.* (2012) A
624 reconciled estimate of ice-sheet mass balance. *Science* 338: 1183-1189.
- 625 Skidmore, M.L., Foght, J.M., and Sharp, M.J. (2000) Microbial life beneath a High Arctic
626 glacier. *Appl Environ Microbiol* 66: 3214-3220.
- 627 Sorokin, Y.I., and Sorokin, P.Y. (1996) Plankton and primary production in the Lena River
628 estuary and in the south-eastern Laptev Sea. *Estuarine Coastal Shelf Sci* 43: 399-418.
- 629 Stibal, M., Hasan, F., Wadham, J.L., Sharp, M.J., and Anesio, A.M. (2012a) Prokaryotic
630 diversity in sediments beneath two polar glaciers with contrasting organic carbon substrates.
631 *Extremophiles* 16: 255-265.
- 632 Stibal, M., Wadham, J.L., Lis, G.P., Telling, J., Pancost, R.D., Dubnick, A., *et al.* (2012b)
633 Methanogenic potential of Arctic and Antarctic subglacial environments with contrasting
634 organic carbon sources. *Glob Chang Biol* 18: 3332–3345.
- 635 Stibal, M., Gözdereliler, E., Cameron, K.A., Box, J.B., Stevens, I.T., Gokul, J.K., *et al.*
636 (2015a) Microbial abundance in surface ice on the Greenland Ice Sheet. *Front Microbiol* 6:
637 225.
- 638 Stibal, M., Schostag, M., Cameron, K.A., Hansen, L.H., Chandler, D.M., Wadham, J.L., and
639 Jacobsen, C.S. (2015b) Different bulk and active bacterial communities in cryoconite from
640 the margin and interior of the Greenland ice sheet. *Environ Microbiol Reports* 7: 293-300.
- 641 Tedesco, M. (2007) A new record in 2007 for melting in Greenland. *Eos, Trans Am Geophys*
642 *Union* 88: 383-383.

- 643 Tedesco, M., Fettweis, X., Mote, T., Wahr, J., Alexander, P., Box, J.E., and Wouters, B.
 644 (2013) Evidence and analysis of 2012 Greenland records from spaceborne observations, a
 645 regional climate model and reanalysis data. *Cryosphere* 7: 615-630.
- 646 Tranter, M., Skidmore, M., and Wadham, J. (2005) Hydrological controls on microbial
 647 communities in subglacial environments. *Hydrol Process* 19: 995-998.
- 648 Wadham, J.L., Tranter, M., Skidmore, M., Hodson, A.J., Priscu, J., Lyons, W.B., *et al.* (2010)
 649 Biogeochemical weathering under ice: size matters. *Glob Biogeochem Cy* 24: GB3025.
- 650 Wadham, J.L., De'ath, R., Monteiro, F.M., Tranter, M., Ridgwell, A., Raiswell, R., and
 651 Tulaczyk, S. (2013) The potential role of the Antarctic Ice Sheet in global biogeochemical
 652 cycles. *Earth Env Sci T R So* 104: 1-13.
- 653 Wilhelm, L., Besemer, K., Fasching, C., Urich, T., Singer, G.A., Quince, C., and Battin, T.J.
 654 (2014) Rare but active taxa contribute to community dynamics of benthic biofilms in glacier-
 655 fed streams. *Environ Microbiol* 16: 2514-2524.
- 656 Yde, J.C., Finster, K.W., Raiswell, R., Steffensen, J.P., Heinemeier, J., Olsen, J., *et al.* (2010)
 657 Basal ice microbiology at the margin of the Greenland ice sheet. *Ann Glaciol* 51: 71-79.

658

659 **Table and Figure legends:**

- 660 Table 1: Analyses of the estimated yearly prokaryotic contribution of C, N and P from LRS,
 661 KRS, the GrIS and the Big-4 Arctic rivers (Yenisey, Lena, Ob and Mackenzie rivers).
 662 Percentage contribution of cellular nutrient refers to the calculated percentage of estimated
 663 annual mass flux of cell associated nutrient relative to total annual mass flux of the nutrient. ^a
 664 - chemistry based on analyses from LRS; ^b - cell abundance based on estimates from LRS; ^c -

665 estimates are based on the lowest values from references; ^d - Hawkings *et al.*, 2014; ^e -
666 measurements made May 9 - October 14; ^f - Fettweis, 2007; ^g - Dittmar & Kattner, 2003; ^h -
667 Lawson *et al.*, 2014b and this study; ⁱ - Wadham *et al.*, submitted, particulate N based on
668 2015 Leverett outflow data ($0.12 \mu\text{g ml}^{-1}$; Kohler, Zarsky, Stibal *et al.*, unpublished), and
669 mean sediment loads from LRS (1.088 g L^{-1} ; Hawkings *et al.*, 2014); ^j - Hawkings *et al.*,
670 2016; ^k - estimated from mean Lena river (Cauwet & Sidorov, 1996) and Mackenzie River
671 (Emmerton *et al.*, 2008) DOP concentrations, and discharge volumes (Dittmar & Kattner,
672 2003); ^l - Sorokin & Sorokin, 1996, Garneau *et al.*, 2006; ^m - percentage based on TOP; ⁿ -
673 percentage based on DOP.

674

675 Fig. 1: Schematic of study site locations (white crosses) within the Kangerlussaq locality, and
676 an inset map of Greenland showing the overall location (black rectangle). Glaciated areas are
677 depicted in white and ice-free areas are depicted in light grey. Watson river and the fjord that
678 it feeds is shown in dark grey. Arrow depicts north.

679

680 Fig. 2 (a) Discharge rates and sediment loads measured at KRS. Black depicts discharge, grey
681 depicts sediment load. Dashed lines indicate sampling days. (b) qPCR 16S rRNA abundance
682 analyses. Grey triangles depict LRS analyses, black circles depict KRS analyses. Error bars
683 depict standard deviations.

684

685 Fig. 3: Box plot with whiskers showing the relative abundance range, median and mean for
686 OTU grouped by phylum-; (a), (b) and order-; (c), (d) level classifications, and by LRS; (a),
687 (c) and KRS; (b), (d) sample sites throughout the sampling period. Grey boxes depict 25th -
688 75th percentiles, whiskers depict maximum and minimum values, box lines depict median
689 values, and cross depicts mean values. Only classifications with $\geq 1\%$ mean relative

690 abundance are shown. Order names in square brackets are suggested annotations from the
691 Greengenes database.

692

693 **Supporting information legends:**

694 Table S1: Sampling dates (day of year 2012) and water volumes (ml) filtered through Sterivex
695 filters at each site. ^a; LRS sample date, ^b; KRS sample date, ^c; outburst event (Hawkings *et al.*,
696 2014), ^d; Leverett and Russell glacial outflow river confluence (LRSc)

697

698 Table S2: Nutrient concentrations of sampled waters (μM). b.d. - below detection. CNFe;
699 colloidal/nanoparticulate Fe. References are depicted with superscript letters; ^a Wadham *et al.*,
700 submitted, ^b Hawkings *et al.*, 2016, ^c Hawkings *et al.*, 2014, ^d Hawkings *et al.*, in review.

701

702 Table S3: Major ion concentrations of sampled waters ($\mu\text{eq l}^{-1}$) from Hawkings *et al.*, 2015.

703

704 Table S4: Particulate P analyses (μM) from Hawkings *et al.*, 2016.

705

706

707

	LRS; 2012	KRS; 2012 ^a	GrIS; 2000 - 2006 ^{a,b}	Big-4 Arctic rivers ^c
Discharge (km ³ yr ⁻¹)	2.2 ^d	6.83 ^e	419.34 ^f	1740 – 1860 ^g
TOC (Mg yr ⁻¹)	5695.51 ^h	17681.98	1.09 x 10 ⁶	1.40 x 10 ⁷ – 1.75 x 10 ⁷ ^g
TON (Mg yr ⁻¹)	329.46 ⁱ	1022.83	62798.18	5.20 x 10 ⁵ – 7.40 x 10 ⁵ ^g
TOP (Mg yr ⁻¹)	72.63 ^j	225.49	13844.09	-
DOP (Mg yr ⁻¹)	2.32 ^j	7.19	441.56	23200 – 38000 ^k
Cells yr ⁻¹ (x10 ²⁰)	1.83	10.25	629.01	>11000 ^l
Estimated cellular C (Mg yr ⁻¹)	5.52	30.95	1900.30	>33200
% contribution of cellular C	0.10	0.18	-	0.24
Estimated cellular N (Mg yr ⁻¹)	1.06	5.94	364.94	>6380
% contribution of cellular N	0.78	1.40	-	1.23
Estimated cellular P (Mg yr ⁻¹)	0.28	1.54	95.01	>1660
% contribution of cellular P	0.38 ^m 12.09 ⁿ	0.68 ^m 21.41 ⁿ	-	>7.15 ⁿ

1 Table 1: Analyses of the estimated yearly prokaryotic contribution of C, N and P from LRS, KRS, the GrIS and
2 the Big-4 Arctic rivers (Yenisey, Lena, Ob and Mackenzie rivers). Percentage contribution of cellular nutrient
3 refers to the calculated percentage of estimated annual mass flux of cell associated nutrient relative to total
4 annual mass flux of the nutrient. ^a - chemistry based on analyses from LRS; ^b - cell abundance based on
5 estimates from KRS; ^c - estimates are based on the lowest values from references; ^d - Hawkings *et al.*, 2014; ^e -
6 measurements made May 9 - October 14; ^f - Fettweis, 2007; ^g - Dittmar & Kattner, 2003; ^h - Lawson *et al.*,
7 2014b and this study; ⁱ - Wadham *et al.*, submitted, particulate N based on 2015 Leverett outflow data (0.12 µg
8 ml⁻¹; Kohler, Zarsky, Stibal *et al.*, unpublished), and mean sediment loads from LRS (1.088 g L⁻¹; Hawkings *et*
9 *al.*, 2014); ^j - Hawkings *et al.*, 2016; ^k - estimated from mean Lena river (Cauwet & Sidorov, 1996) and
10 Mackenzie River (Emmerton *et al.*, 2008) DOP concentrations, and discharge volumes (Dittmar & Kattner,

11 2003); ^l - Sorokin & Sorokin, 1996, Garneau *et al.*, 2006; ^m - percentage based on TOP; ⁿ - percentage based on

12 DOP.

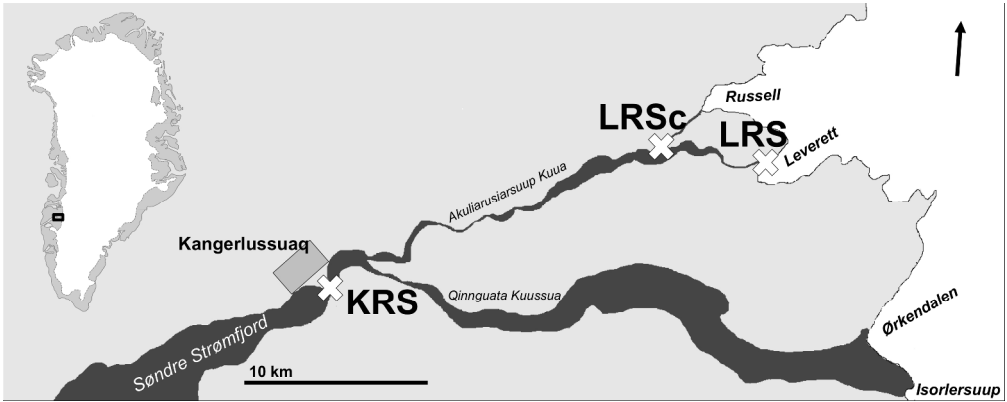


Fig. 1: Schematic of study site locations (white crosses) within the Kangerlussuaq locality, and an inset map of Greenland showing the overall location (black rectangle). Glaciated areas are depicted in white and ice-free areas are depicted in light grey. Watson river and the fjord that it feeds is shown in dark grey. Arrow depicts north.

Fig. 1

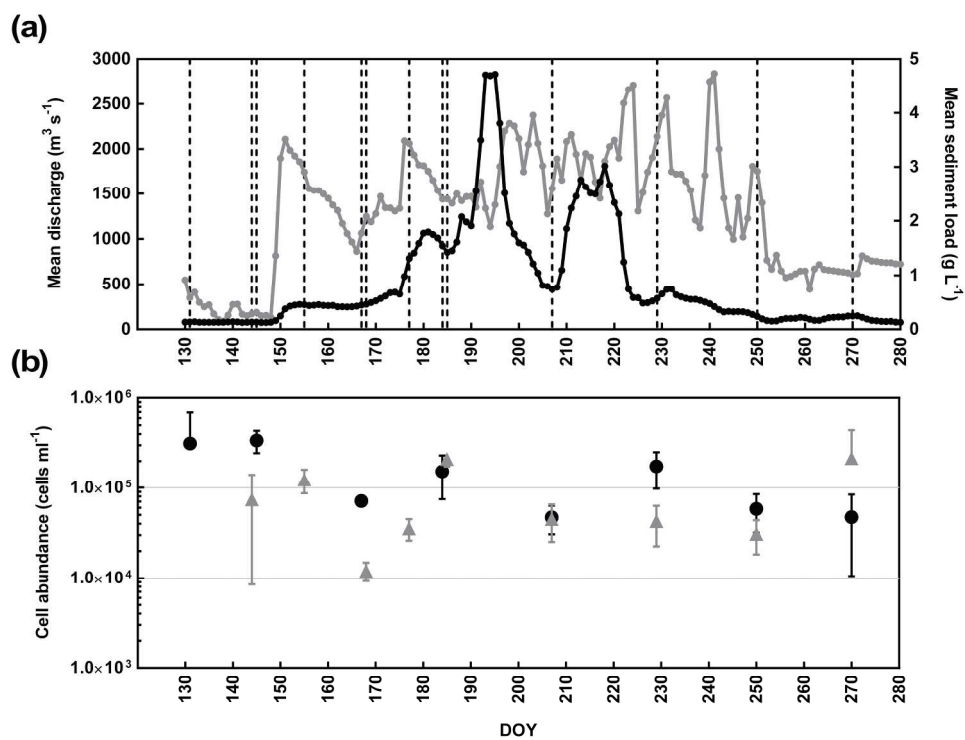


Fig. 2 (a) Discharge rates and sediment loads measured at KRS. Black depicts discharge, grey depicts sediment load. Dashed lines indicate sampling days. (b) qPCR 16S rRNA abundance analyses. Grey triangles depict LRS analyses, black circles depict KRS analyses. Error bars depict standard deviations.

Fig. 2
232x180mm (300 x 300 DPI)

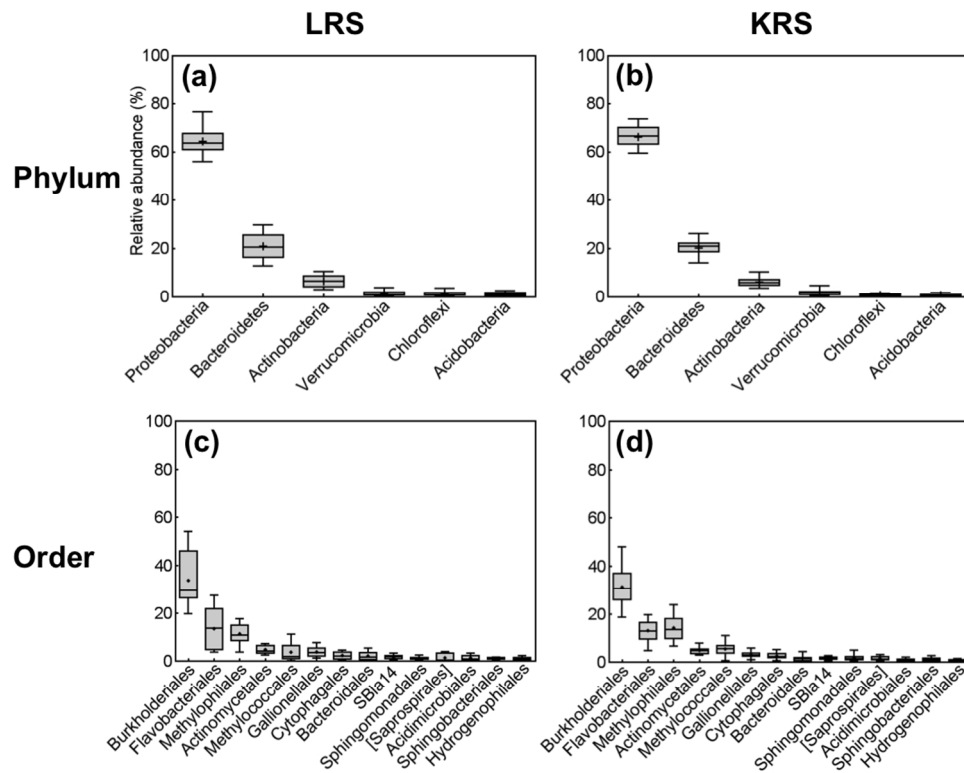


Fig. 3: Box plot with whiskers showing the relative abundance range, median and mean for OTU grouped by phylum-; (a), (b) and order-; (c), (d) level classifications, and by LRS; (a), (c) and KRS; (b), (d) sample sites throughout the sampling period. Grey boxes depict 25th - 75th percentiles, whiskers depict maximum and minimum values, box lines depict median values, and cross depicts mean values. Only classifications with $\geq 1\%$ mean relative abundance are shown. Order names in square brackets are suggested annotations from the Greengenes database.

Fig. 3